Marine and Maritime Intelligent Robotics

Andreas SITORUS

Worachit KETRUNGSRI

Underwater Robotics, Modeling and Control

Modeling and Control of Underwater Vehicle: Sparus

January 15, 2023

University of Toulon

Contents

List of Figures

Chapter 1

Introduction

1.1 Background

The purpose of this document is to model the parameter for the dynamic equation of the Sparus AUV. The documents also contained the verification of the parameters via simulation in MATLAB.

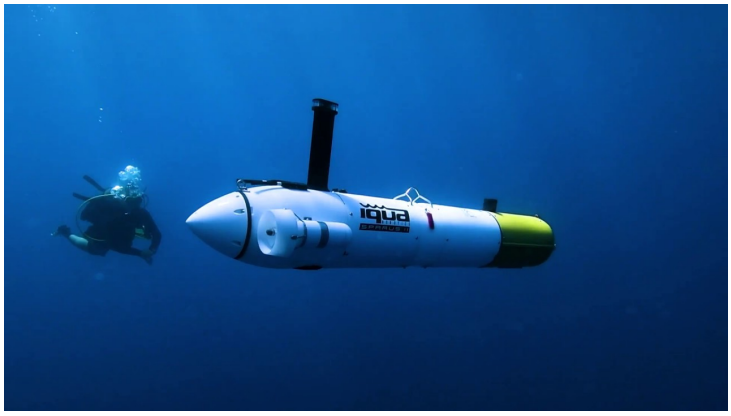

Figure 1.1: Sparus AUV on Mission

1.2 Sparus Main Characteristics

The origin frame of the Sparus (F_b) is defined at the middle of the system. The x-axis of F_b is placed in the middle of the two thruster and point toward the hemisphere part of the Sparus while the z-axis point toward the opposite side of the antenna as show in figure 1.2.

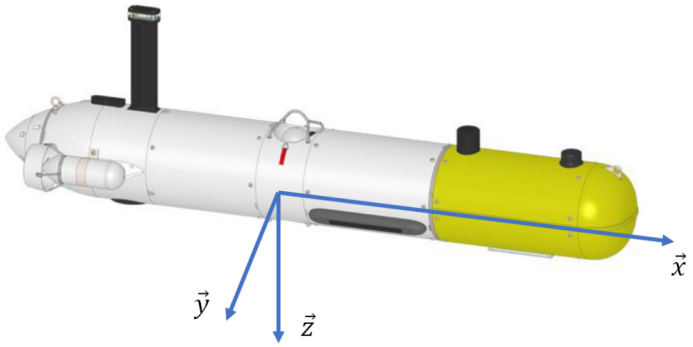

Figure 1.2: Sparus model with the origin frame (F_b)

In this document, we define the origin of the Sparus body to be the same as the center of gravity of the model, resulting in the (1.1). The distance from the origin of F_b to the center of buoyancy is given in (1.2)

$$\mathbf{r}_{cg}^{b} = \begin{bmatrix} 0 \\ 0 \\ 0 \end{bmatrix} \text{m} \tag{1.1}$$

$$\mathbf{r}_{bu}^{b} = \begin{bmatrix} 0 \\ 0 \\ -0.02 \end{bmatrix} \text{m} \tag{1.2}$$

Chapter 2

Dynamic Modeling

2.1 Kinematics

The state of the system is define in the F_b consist of two main vectors, the linear velocity ($\boldsymbol{\eta}$) and the angular velocity ($\boldsymbol{\omega}$)

$$\begin{aligned} \mathbf{v}^b &= \begin{bmatrix} \boldsymbol{\eta}^b \\ \boldsymbol{\omega}^b \end{bmatrix} \\ &= \begin{bmatrix} \dot{x} & \dot{y} & \dot{z} & \dot{p} & \dot{q} & \dot{r} \end{bmatrix}^\top \end{aligned} \tag{2.1}$$

where:

$\mathbf{v}^b_{cg}$ is the speed of the vehicle within frame b (F_b). This variable is the state variable of the system.

$\boldsymbol{\eta} = \langle \dot{x}, \dot{y}, \dot{z} \rangle$ is the speed of the vehicle in x, y, z axis with respect to the F_b.

$\boldsymbol{\omega} = \langle \dot{p}, \dot{q}, \dot{r} \rangle$ is the angular rotation around axis x, y, z of F_b.

The transformation of the velocity in the reference frame (F_b) to the initial frame (F_e) can be done using the transfer matrix $J(\Theta)$.

$$\begin{aligned} \boldsymbol{\Theta} &= \langle p, q, r \rangle \\ \mathbf{v}^e &= J(\boldsymbol{\Theta})\mathbf{v}^b \\ &= \begin{bmatrix} R(\Theta) & [0]_{3\times3} \\ [0]_{3\times3} & T(\Theta) \end{bmatrix} \mathbf{v}^b \end{aligned} \tag{2.2}$$

2.2 Dynamics

The dynamic equation of the system in F_b is specified in (2.3)

$$(M_B^b + M_A^b)\dot{\mathbf{v}} + C_G^b\mathbf{v} = \mathbf{G}^b - \mathbf{B}^b - \mathbf{K}^b - \mathbf{U}^b \tag{2.3}$$

where:

M_B^b is the body mass matrix

M_A^b is the added mass matrix

C_G^b is the generalized Coriolis matrix

$\mathbf{G}^b$ is the gravity vector

$\mathbf{B}^b$ is the buoyancy vector

$\mathbf{K}^b$ is the friction vector

$\mathbf{U}^b$ is the thrust mapped vector

Chapter 3

Parameter identification

3.1 Sparus Dimension

Before we estimated the parameters of the robots, we must measure the dimensions of the SPARUS. This is done based on the assumption that

- The dimension of the SPARUS can be measured from the given images (figure 3.1).
- The mass is equally distributed (the density of the robot is constant).

Figure 3.1: Sparus AUV from top, front, and side view

The dimension of the Sparus is define using the variables show in figure 3.2 and the values of each variable together with the type of the three-dimensional geometric shapes are shown in table 3.1. The origin frame (F_b) is located at the middle of the main body. The table 3.1 also contained the position vector from the origin of F_b to the center-of-mass of each geometric

shape ($\mathbf{p}_i^b$).

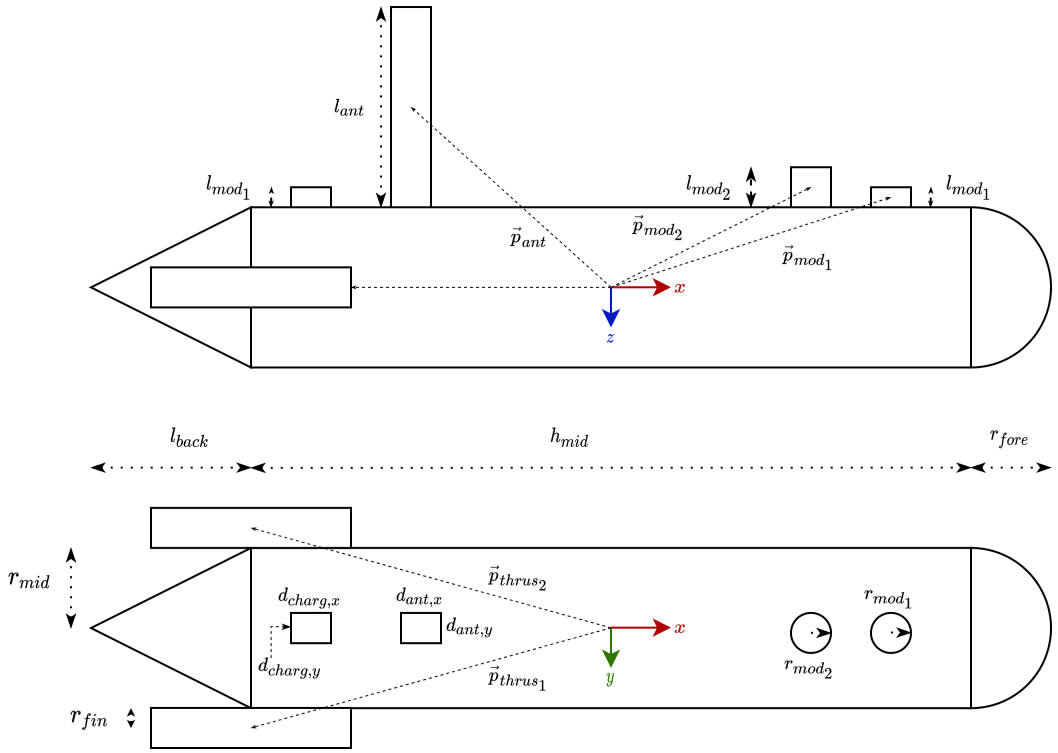

Figure 3.2: Sparus AUV drawing with variables

3.2 Volume and Mass

To compute the mass and inertia of each body, the mass is assume to be equally distribute (the density is constant throughout the body) and the calculation will not take into account the mass of the internal component of the Sparus. The total mass (m_{total}) of the Sparus is 52 kg.

$$
\begin{aligned}
V_{head} &= \frac{2}{3}\pi r_{head}^3 \\
V_{mid} &= \pi r_{mid}^2 l_{mid} \\
V_{back} &= \frac{1}{3}\pi r_{back}^2 l_{back} \\
V_{thrus} &= \pi r_{thrus}^2 l_{thrus} \\
V_{mod_1} &= \pi r_{mod_1}^2 l_{mod_1} \\
V_{mod_2} &= \pi r_{mod_2}^2 l_{mod_2} \\
V_{ant} &= d_{ant,x} d_{ant,y} l_{ant} \\
V_{charg} &= d_{charg,x} d_{charg,y} l_{charg}
\end{aligned}
\tag{3.1}
$$

Dimensional Parameters	Value (m)
Forepart of the main body (hemisphere)	
r_{fore}	0.115
$\mathbf{p}^b_{fore}$	$\langle 0.7381, 0, 0\rangle$
Middle part of the main body (cylinder)	
l_{mid}	1.245
r_{mid}	0.115
$\mathbf{p}^b_{mid}$	$\langle 0.0675, 0, 0\rangle$
Back part of the main body (cone)	
l_{back}	0.24
r_{back}	0.115
$\mathbf{p}^b_{back}$	$\langle -0.6200, 0, 0\rangle$
Thruster (cylinder)	
l_{thrus}	0.231
r_{thrus}	0.05
$\mathbf{p}^b_{thrus_1}$	$\langle -0.59, -0.17, 0\rangle$
$\mathbf{p}^b_{thrus_2}$	$\langle -0.59, 0.17, 0\rangle$
Modem 1 (cylinder)	
h_{mod_1}	0.023
r_{mod_1}	0.023
$\mathbf{p}^b_{mod_1}$	$\langle 0.6380, 0, 0.1265\rangle$
Modem 2 (cylinder)	
l_{mod_2}	0.05
r_{mod_2}	0.023
$\mathbf{p}^b_{mod_2}$	$\langle 0.3710, 0, 0.1400\rangle$
Antenna (rectangular prism)	
l_{ant}	0.2415
$d_{ant,x}$	0.069
$d_{ant,y}$	0.0345
$\mathbf{p}^b_{ant}$	$\langle -0.4530, 0, 0.2358\rangle$
Charger (rectangular prism)	
l_{charg}	0.0115
$d_{charg,x}$	0.069
$d_{charg,y}$	0.023
$\mathbf{p}^b_{charg}$	$\langle -0.5550, 0, 0.1208\rangle$

Table 3.1: The table shows the variable and value of the Sparus's dimensional parameters

The total mass (3.2) of the system is the summation of all the bodies from (3.1). Note that the volume of both thruster are equal.

$$\begin{aligned} V_{total} &= \sum_i V_i \\ &= V_{fore} + V_{mid} + V_{back} + 2V_{thrus} \\ &+ V_{mod_1} V_{mod_2} + V_{ant} + V_{charg} \end{aligned} \tag{3.2}$$

To compute the mass of each object (m_i), we need to compute the average density of the total body (3.3). Then, since the density of each object is equally distribute, the mass of each object can be obtained from the formula in (3.1)

$$\rho_{total} = \frac{m_{total}}{V_{total}} \tag{3.3}$$

$$m_i = \rho_{total} V_i \tag{3.4}$$

The resulting mass and volume of each part after the parameters' substitution from the table 3.1 is shown in table 3.2.

3.3 Inertia

To obtain the total inertia of the system, we need to first obtain the inertia of each part of the Sparus. Since each parts of the model can be considered as simple 3D geometric shape, the inertia formula of this shape can be obtained without the use of numerical integration. The formula of the 3D geometric shapes that will be used is list in (3.5). The inertia formula of $I_{i,j}(\cdot)$ means that it's the formula of i shape with j as a main axis. The origin of these inertia matrix formula is at the center-of-gravity of each body with the same axes direction as F_b.

$$
\begin{aligned}
I_{hemisphere,x}\left(m,r\right) &= \begin{bmatrix} \frac{2}{5}mr^2 & 0 & 0 \\ 0 & \frac{83}{320}mr^2 & 0 \\ 0 & 0 & \frac{83}{320}mr^2 \end{bmatrix} \\
I_{cylinder,x}\left(m,r,l\right) &= \begin{bmatrix} m\frac{r^2}{2} & 0 & 0 \\ 0 & m\left(\frac{r^2}{4}+\frac{l^2}{12}\right) & 0 \\ 0 & 0 & m\left(\frac{r^2}{4}+\frac{l^2}{12}\right) \end{bmatrix} \\
I_{cylinder,z}\left(m,r,l\right) &= \begin{bmatrix} m\left(\frac{r^2}{4}+\frac{l^2}{12}\right) & 0 & 0 \\ 0 & m\left(\frac{r^2}{4}+\frac{l^2}{12}\right) & 0 \\ 0 & 0 & m\frac{r^2}{2} \end{bmatrix} \\
I_{cone,x}\left(m,r,l\right) &= \begin{bmatrix} \frac{3}{10}mr^2 & 0 & 0 \\ 0 & m\left(\frac{3}{20}r^2+\frac{3}{80}l^2\right) & 0 \\ 0 & 0 & m\left(\frac{3}{20}r^2+\frac{3}{80}l^2\right) \end{bmatrix} \\
I_{\text{prism},z}\left(m,d_1,d_2,l\right) &= \begin{bmatrix} \frac{1}{12}m\left(d_2^2+l^2\right) & 0 & 0 \\ 0 & \frac{1}{12}m\left(d_1^2+l^2\right) & 0 \\ 0 & 0 & \frac{1}{12}m\left(d_1^2+d_2^2\right) \end{bmatrix}
\end{aligned}
\tag{3.5}
$$

From the type of shape specified in table 3.1 and the formula in (3.5), the inertia of each part of the Sparus are shown in (3.6).

$$
\begin{aligned}
I_{fore} &= I_{hemisphere,x}(m_{fore}, r_{fore}) \\
I_{mid} &= I_{cylinder,x}(m_{mid}, r_{mid}, l_{mid}) \\
I_{back} &= I_{cone,x}(m_{back}, r_{back}) \\
I_{thrus} &= I_{cylinder,x}(m_{thrus}, r_{thrus}, l_{thrus}) \\
I_{mod_1} &= I_{cylinder,z}(m_{mod_1}, r_{mod_1}, l_{mod_1}) \\
I_{mod_2} &= I_{cylinder,z}(m_{mod_2}, r_{mod_2}, l_{mod_2}) \\
I_{ant} &= I_{prism,z}(m_{ant}, d_{ant,x}, d_{ant,y}, l_{ant}) \\
I_{charg} &= I_{prism,z}(m_{charg}, d_{charg,x}, d_{charg,y}, l_{charg})
\end{aligned}
\tag{3.6}
$$

The resulting inertia matrix of each part after the parameters' substitution from the table 3.1 is also shown in table 3.2. The $diag(\cdot)$ is the diagonal matrix define in (3.7)

$$diag(a_1, ..., a_n) = \mathbb{I}_{n\times n} \begin{bmatrix} a_1 \\ \vdots \\ a_n \end{bmatrix} \tag{3.7}$$

where:

$\mathbb{I}_{n\times m}$ is the identity matrix with $n \times m$ dimension.

Dimensional Parameters	Value
Forepart of the main body	
m_{fore}	$0.3463\,\mathrm{kg}$
V_{fore}	$3.9816 \times 10^{-4}\,\mathrm{m}^3$
I_{fore}	$diag(0.0018, 0.0012, 0.0012)\,\mathrm{kg\,m}^2$
Middle part of the main body	
m_{mid}	$44.9860\,\mathrm{kg}$
V_{mid}	$0.0517\,\mathrm{m}^3$
I_{mid}	$diag(0.2975, 5.9595, 5.9595)\,\mathrm{kg\,m}^2$
Back part of the main body	
m_{back}	$2.8907\,\mathrm{kg}$
V_{back}	$0.0033\,\mathrm{m}^3$
I_{back}	$diag(0.0115, 0.0120, 0.0120)\,\mathrm{kg\,m}^2$
Thruster	
m_{thrus}	$1.5778\,\mathrm{kg}$
V_{thrus}	$0.0018\,\mathrm{m}^3$
I_{thrus}	$diag(0.002, 0.008, 0.008)\,\mathrm{kg\,m}^2$
Modem 1	
m_{mod_1}	$0.0332\,\mathrm{kg}$
V_{mod_1}	$3.8224 \times 10^{-5}\,\mathrm{m}^3$
I_{mod_1}	$diag(0.8793\mathrm{e}{-5}, 0.5862\mathrm{e}{-5}, 0.5862\mathrm{e}{-5})\,\mathrm{kg\,m}^2$
Modem 2	
m_{mod_2}	$0.0723\,\mathrm{kg}$
V_{mod_2}	$8.3095 \times 10^{-5}\,\mathrm{m}^3$
I_{mod_2}	$diag(0.1911\mathrm{e}{-4}, 0.2461\mathrm{e}{-4}, 0.2461\mathrm{e}{-4})\,\mathrm{kg\,m}^2$
Antenna	
m_{ant}	$0.5000\,\mathrm{kg}$
V_{ant}	$5.7489 \times 10^{-4}\,\mathrm{m}^3$
I_{ant}	$diag(0.0025, 0.0026, 0.0002)\,\mathrm{kg\,m}^2$
charger	
m_{charg}	$0.0159\,\mathrm{kg}$
V_{charg}	$1.8251 \times 10^{-5}\,\mathrm{m}^3$
I_{charg}	$diag(0.0875\mathrm{e}{-5}, 0.6472\mathrm{e}{-5}, 0.6997\mathrm{e}{-5})\,\mathrm{kg\,m}^2$
Entire body	
m_{total}	$52\,\mathrm{kg}$
ρ_{total}	$869.6862\,\mathrm{kg\,m}^{-3}$
V_{total}	$0.0598\,\mathrm{m}^3$

Table 3.2: The table shows the variable and value of the Sparus's parameters

Chapter 4

Modeling

4.1 Global Body Mass Matrix

The body mass matrix (M_B^b) is the 6×6 matrix which depends on the total mass and inertia, but does not depend on the state of the system. The body mass matrix of each body ($M_{B,i}^{cg_i}$) can be formulated using (4.1) where i is the name of each part of Sparus and the origin of the frame of reference is at the center-of-gravity of each body (cg_i).

$$M_{B,i}^{cg_i} = \begin{bmatrix} m_i \mathbb{I}_{3\times 3} & [0]_{3\times 3} \\ [0]_{3\times 3} & I_i \end{bmatrix} \tag{4.1}$$

In order to simulate the movement of the system, we must compute the total mass matrix of the system ($M_{B,total}^b$). However, we cannot directly add the mass matrix on each part together because the origin frame of each inertia matrix is different (even though the direction of each axis is the same). To translate the origin frame of each mass matrix from the respective center of gravity (cg_i) to the origin of F_b, we must use (4.20).

$$M_{B,i}^b = \begin{bmatrix} \mathbb{I}_{3\times 3} & [0]_{3\times 3} \\ S(\mathbf{r}_{cg_i}^b) & \mathbb{I}_{3\times 3} \end{bmatrix} M_{B,i}^{cg_i} \begin{bmatrix} \mathbb{I}_{3\times 3} & S^\top(\mathbf{r}_{cg_i}^b) \\ [0]_{3\times 3} & \mathbb{I}_{3\times 3} \end{bmatrix} \tag{4.2}$$

where:

$[0]_{n\times m}$ is the zero matrix with $n \times m$ dimension.

$S(\mathbf{r}^b_{cg_i})$ is the skew-symmetric matrix specified in (4.3). Note that the multiplication between a skew matrix and a vector is a cross product between two vectors ($S^\top(\mathbf{a})\mathbf{b} = a \times b$).

$$S(\mathbf{r}) = \begin{bmatrix} 0 & -r_3 & r_2 \\ r_3 & 0 & -r_1 \\ -r_2 & r_1 & 0 \end{bmatrix}, \mathbf{r} \in \mathbb{R}^3 \tag{4.3}$$

By substituting the value from the table 3.1 and 3.2, the numerical solution of each inertia matrix can be obtained.

$$
\begin{aligned}
M^b_{B,head} &= \begin{bmatrix} 0.3463 & 0 & 0 & 0 & 0 & 0 \\ 0 & 0.3463 & 0 & 0 & 0 & 0.2556 \\ 0 & 0 & 0.3463 & 0 & -0.2556 & 0 \\ 0 & 0 & 0 & 0.0018 & 0 & 0 \\ 0 & 0 & -0.2556 & 0 & 0.1898 & 0 \\ 0 & 0.2556 & 0 & 0 & 0 & 0.1898 \end{bmatrix} \\
M^b_{B,mid} &= \begin{bmatrix} 44.9860 & 0 & 0 & 0 & 0 & 0 \\ 0 & 44.9860 & 0 & 0 & 0 & 3.0366 \\ 0 & 0 & 44.9860 & 0 & -3.0366 & 0 \\ 0 & 0 & 0 & 0.2975 & 0 & 0 \\ 0 & 0 & -3.0366 & 0 & 6.1645 & 0 \\ 0 & 3.0366 & 0 & 0 & 0 & 6.1645 \end{bmatrix} \\
M^b_{B,back} &= \begin{bmatrix} 2.8907 & 0 & 0 & 0 & 0 & 0 \\ 0 & 2.8907 & 0 & 0 & 0 & -2.3125 \\ 0 & 0 & 2.8907 & 0 & 2.3125 & 0 \\ 0 & 0 & 0 & 0.0115 & 0 & 0 \\ 0 & 0 & 2.3125 & 0 & 1.9557 & 0 \\ 0 & -2.3125 & 0 & 0 & 0 & 1.9557 \end{bmatrix} \\
M^b_{B,mod_1} &= \begin{bmatrix} 0.0332 & 0 & 0 & 0 & 0.0042 & 0 \\ 0 & 0.0332 & 0 & -0.0042 & 0 & 0.0212 \\ 0 & 0 & 0.0332 & 0 & -0.0212 & 0 \\ 0 & -0.0042 & 0 & 0.0005 & 0 & -0.0027 \\ 0.0042 & 0 & -0.0212 & 0 & 0.0141 & 0 \\ 0 & 0.0212 & 0 & -0.0027 & 0 & 0.0135 \end{bmatrix} \\
M^b_{B,mod_2} &= \begin{bmatrix} 0.0723 & 0 & 0 & 0 & 0.0101 & 0 \\ 0 & 0.0723 & 0 & -0.0101 & 0 & 0.0268 \\ 0 & 0 & 0.0723 & 0 & -0.0268 & 0 \\ 0 & -0.0101 & 0 & 0.0014 & 0 & -0.0038 \\ 0.0101 & 0 & -0.0268 & 0 & 0.0114 & 0 \\ 0 & 0.0268 & 0 & -0.0038 & 0 & 0.0100 \end{bmatrix}
\end{aligned} \tag{4.4}
$$

$$M^b_{B,ant} = \begin{bmatrix} 0.5000 & 0 & 0 & 0 & 0.1179 & 0 \\ 0 & 0.5000 & 0 & -0.1179 & 0 & -0.2265 \\ 0 & 0 & 0.5000 & 0 & 0.2265 & 0 \\ 0 & -0.1179 & 0 & 0.0303 & 0 & 0.0534 \\ 0.1179 & 0 & 0.2265 & 0 & 0.1330 & 0 \\ 0 & -0.2265 & 0 & 0.0534 & 0 & 0.1028 \end{bmatrix}$$

$$M^b_{B,charg} = \begin{bmatrix} 0.0159 & 0 & 0 & 0 & 0.0019 & 0 \\ 0 & 0.0159 & 0 & -0.0019 & 0 & -0.0088 \\ 0 & 0 & 0.0159 & 0 & 0.0088 & 0 \\ 0 & -0.0019 & 0 & 0.0002 & 0 & 0.0011 \\ 0.0019 & 0 & 0.0088 & 0 & 0.0051 & 0 \\ 0 & -0.0088 & 0 & 0.0011 & 0 & 0.0049 \end{bmatrix}$$

Lastly, the total body mass matrix is computed from the summation of the transform coordinate matrix specify in (4.4)

$$\begin{aligned} M^b_{B,total} &= \sum_i M^b_{B,i} \\ &= \begin{bmatrix} 52.0000 & 0 & 0 & 0 & 0.1341 & 0 \\ 0 & 52.0000 & 0 & -0.1341 & 0 & -1.0695 \\ 0 & 0 & 52.0000 & 0 & 1.0695 & 0 \\ 0 & -0.1341 & 0 & 0.4384 & 0 & 0.0480 \\ 0.1341 & 0 & 1.0695 & 0 & 9.5881 & 0 \\ 0 & -1.0695 & 0 & 0.0480 & 0 & 9.6470 \end{bmatrix} \end{aligned} \tag{4.5}$$

4.2 Global Added Mass Matrix

The added mass matrix or the virtual mass ($M_A \in \mathbb{R}^{6\times6}$) is the added inertia of the system due to the fluid flow around the object. This effect happens when the object accelerates under the fluid, which cause the increasing in the total inertia of the system. Normally, to obtain this matrix, we must perform the numerical simulation using Navier Stroke equation in software. However, for simplicity, the analytical solution such as Slender body theorem and Lamb's k-factors for spheroid are used to approximate the added mass matrix. The parameters that will

be used in this section came from the dimension and object properties from chapter 3. In this section, we demonstrate the method that used to compute the added mass of the main body ($M_{A,main}$). We also show the result of other added mass matrix such as the added mass for thrusters ($M_{A,thrus}$) and antenna ($M_{A,ant}$). These matrices are compared with the $M_{A,main}$ to show the significance of each additional added mass.

4.2.1 Main body added mass ($M_{A,main}$)

The main body of the Sparus can be simplified into 3 simple 3D geometrics shapes as shown in figure 4.1 1. The hemispherical head section 2. The cylindrical middle section 3. The conic back section.

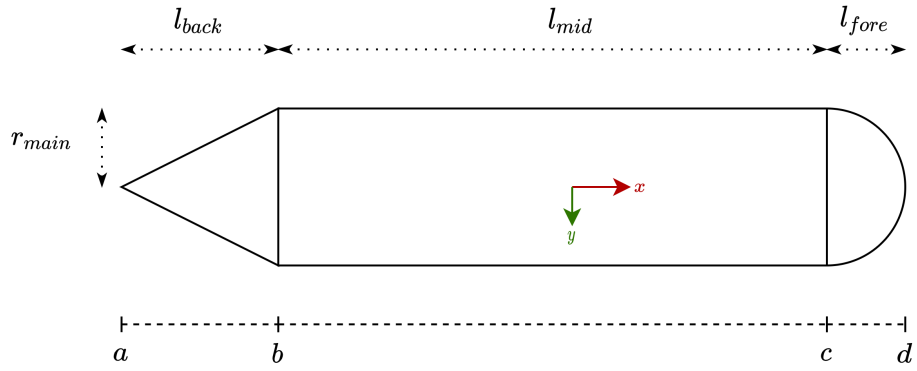

Figure 4.1: Dimension of the main body of the Sparus

From figure 4.1, we can derive the equation for the location of each point in the body fixed frame (F_b) coordinate. The equations given in (4.6) will be used to compute the added mass matrix in the further section.

$$\begin{aligned} a &= -l_{back} + \frac{-l_{mid} - l_{back} - r_{fore}}{2} \\ b &= \frac{-l_{mid} - l_{back} - r_{fore}}{2} \\ c &= \frac{l_{mid} - l_{back} - r_{fore}}{2} \\ d &= r_{fore} + \frac{l_{mid} - l_{back} - r_{fore}}{2} \end{aligned} \tag{4.6}$$

The main body of the Sparus from the combining simple geometric shape is in the two-plane symmetries; Therefore, the added mass matrix can be simplified as show in (4.7).

$$M^b_{A,main} = \begin{bmatrix} m_{A,11} & 0 & 0 & 0 & 0 & 0 \\ 0 & m_{A,22} & 0 & 0 & 0 & m_{A,26} \\ 0 & 0 & m_{A,33} & 0 & m_{A,26} & 0 \\ 0 & 0 & 0 & m_{A,44} & 0 & 0 \\ 0 & 0 & m_{A,53} & 0 & m_{A,55} & 0 \\ 0 & m_{A,62} & 0 & 0 & 0 & m_{A,66} \end{bmatrix} \tag{4.7}$$

Firstly, the slender body theorem is used to identify every component of the matrix **except** $m_{A,11}$. The slender body can be applied when the object has the length in one dimension significantly longer than the length in the other dimension. It used the two-dimensional added mass coefficient of the sectional body to compute the 3D mass coefficient. The theory state that

$$\begin{aligned} m_{A,22} &= \int_L a_{22}\, dx \\ m_{A,33} &= \int_L a_{33}\, dx \\ m_{A,44} &= \int_L a_{44}\, dx \\ m_{A,55} &= \int_L x^2 a_{22}\, dx \\ m_{A,66} &= \int_L x^2 a_{33}\, dx \\ m_{A,26} = m_{A,62} &= \int_L a_{22}\, dx \\ m_{A,35} = m_{A,53} &= \int_L a_{33}\, dx \end{aligned} \tag{4.8}$$

where:

a_{22} is the 2D mass coefficient due to a force from a unit acceleration in y-direction.

a_{33} is the 2D mass coefficient due to a force from a unit acceleration in z-direction.

a_{44} is the 2D mass coefficient due to a moment from a unit rotational acceleration about x-axis

For the simplified model of Sparus, the 2D cross-section of the main body is the circle with varied radius depends on the sections. This sectional coefficient is defined as

$$\begin{aligned} a_{22} &= \pi r^2 \\ a_{33} &= \pi r^2 \\ a_{44} &= 0 \end{aligned} \tag{4.9}$$

Before calculating the integration on each main body section, we must obtain the function of radius on each part that depends on the position in the x-axis ($R(x)$). For the forepart of the main body, we can use the similar triangle theorem

$$\frac{R_{back}(x)}{x-a} = \frac{r_{back}}{l_{back}} \tag{4.10}$$

$$R_{back}(x) = \left(\frac{x-a}{l_{back}} r_{back}\right) \tag{4.11}$$

For the hemisphere part, we used the equation of circle that has the center at (c_x, c_y), and using the boundary condition specify in (4.6) as a center of the circle resulting in (4.13).

$$(y-c_y)^2 = r^2 - (x-c_x)^2 \tag{4.12}$$

$$R_{fore}(x) = \sqrt{r_{fore}^2 - (x-c)^2} \tag{4.13}$$

where:

a, d is the boundary of main body section from (4.6)

Since, the circle is the symmetry object, resulting in the equal value of 2D coefficient in y and z direction ($a_{22} = a_{33}$) and the coefficient due to the moment around x-axis equal to 0. Using the equation from (4.6) to (4.13), we obtained the coefficients of the added mass matrix

$$
\begin{aligned}
m_{A,22} = m_{A,33} &= \int_a^b \pi R_{tail}^2(x)\,dx + \int_b^c \pi r_{mid}^2\,dx + \int_c^d \pi R_{fore}^2(x)\,dx \\
m_{A,44} &= 0 \\
m_{A,55} = m_{A,66} &= \int_a^b x^2\pi R_{tail}^2(x)\,dx + \int_b^c x^2\pi r_{mid}^2\,dx + \int_c^d x^2\pi R_{fore}^2(x)\,dx \\
m_{A,26} = m_{A,62} &= \int_a^b x\pi R_{tail}^2(x)\,dx + \int_b^c x\pi r_{mid}^2\,dx + \int_c^d x\pi R_{fore}^2(x)\,dx \\
m_{A,35} = m_{A,53} &= -\int_a^b x\pi R_{tail}^2(x)\,dx - \int_b^c x\pi r_{mid}^2\,dx - \int_c^d x\pi R_{fore}^2(x)\,dx
\end{aligned}
\tag{4.14}
$$

By substituting the parameters from chapter 3, we get

$$
\begin{aligned}
m_{A,22} = m_{A,33} &= 11 \\
m_{A,44} &= 0 \\
m_{A,55} = m_{A,66} &= 11 \\
m_{A,26} = m_{A,62} &= 11 \\
m_{A,35} = m_{A,53} &= 11
\end{aligned}
\tag{4.15}
$$

Secondly, to analytically compute the 3D coefficient due to the force from acceleration in x-direction ($m_{A,11}$), we can use another theorem called "Lamb's k-factors theorem""to approximate this value. The theorem model the 3D object as a spheroid (figure 4.2) and by using this simplified shape instead of the shape specify in figure 4.1, $m_{A,11}$ can be computed from the equations (4.16).

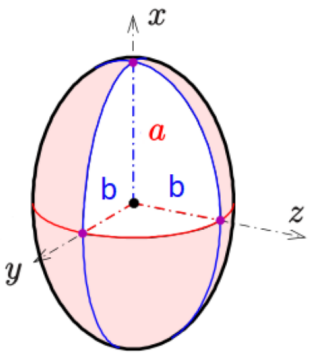

Figure 4.2: The figure show the spheroid shape for k-factors theorem

$$
\begin{aligned}
m_{df} &= \frac{4}{3}\rho\pi b^2 a \\
e &= \sqrt{1-\frac{b^2}{a^2}} \\
\alpha_0 &= 2\frac{1-e^2}{e^3}\left(\frac{1}{2}\ln\left[\frac{1+e}{1-e}\right]-e\right) \\
k_1 &= \frac{\alpha_0}{2-\alpha_0} \\
m_{A,11} &= k_1 m_{df}
\end{aligned}
\tag{4.16}
$$

where:

a is the radius along the major axis of prolate spheroid, $a = \frac{l_{back}+l_{mid}+r_{fore}}{2}$

b is the radius along the minor axis of prolate spheroid, $b = r_{mid}$

From the equations given in (4.16), we substitute the values from chapter 3 to get

$$
m_{A,11} = 11 \tag{4.17}
$$

Lastly, the numerical solution for the added mass matrix from the main body ($M_{A,main}$) is

$$
M_{A,main} = \begin{bmatrix}
1.3948 & 0 & 0 & 0 & 0 & 0 \\
0 & 58.2335 & 0 & 0 & 0 & 2.8842 \\
0 & 0 & 85.1083 & 0 & 12.7371 & 0 \\
0 & 0 & 0 & -0.0952 & 0 & 0 \\
0 & 0 & 12.7371 & 0 & 19.5174 & 0 \\
0 & 2.8842 & 0 & 0 & 0 & 9.7774
\end{bmatrix}
\tag{4.18}
$$

4.2.2 Added mass of other parts

The added mass matrix on other parts used the same method as we used to compute the added mass of the main body. The numerical result is shown in 4.19

$$
\begin{aligned}
M^b_{B,mod_1} &= \begin{bmatrix}
0.0255 & 0 & 0 & 0 & 0.0032 & 0 \\
0 & 0.0255 & 0 & -0.0032 & 0 & 0.0163 \\
0 & 0 & 0 & 0 & 0 & 0 \\
0 & -0.0032 & 0 & 0.0004 & 0 & -0.0021 \\
0.0032 & 0 & 0 & 0 & 0.0004 & 0 \\
0 & 0.0163 & 0 & -0.0021 & 0 & 0.0104
\end{bmatrix} \\
M^b_{B,mod_2} &= \begin{bmatrix}
0.0255 & 0 & 0 & 0 & 0.0036 & 0 \\
0 & 0.0255 & 0 & -0.0036 & 0 & 0.0095 \\
0 & 0 & 0 & 0 & 0 & 0 \\
0 & -0.0036 & 0 & 0.0005 & 0 & -0.0013 \\
0.0036 & 0 & 0 & 0 & 0.0005 & 0 \\
0 & 0.0095 & 0 & -0.0013 & 0 & 0.0035
\end{bmatrix} \\
M^b_{B,ant} &= \begin{bmatrix}
0.8434 & 0 & 0 & 0 & 0.1988 & 0 \\
0 & 3.1498 & 0 & -0.7426 & 0 & -1.4269 \\
0 & 0 & 0.2185 & 0 & 0.0990 & 0 \\
0 & -0.7426 & 0 & 0.1751 & 0 & 0.3364 \\
0.1988 & 0 & 0.0990 & 0 & 0.1068 & 0 \\
0 & -1.4269 & 0 & 0.3364 & 0 & 0.6615
\end{bmatrix} \\
M^b_{B,charg} &= \begin{bmatrix}
0.0111 & 0 & 0 & 0 & 0.0013 & 0 \\
0 & 0.0996 & 0 & -0.0120 & 0 & -0.0553 \\
0 & 0 & 0.0372 & 0 & 0.0207 & 0 \\
0 & -0.0120 & 0 & 0.0015 & 0 & 0.0067 \\
0.0013 & 0 & 0.0207 & 0 & 0.0117 & 0 \\
0 & -0.0553 & 0 & 0.0067 & 0 & 0.0308
\end{bmatrix}
\end{aligned}
\tag{4.19}
$$

4.2.3 Total added mass

Since the behavior of the added mass matrix is the same as the body mass matrix, the added mass that obtained from the section 4.2.2 also need to be applied the transformation from the frame which has the origin at the gravity center of solid (F_{cg_i}) to F_b. The transformation can be done using the same equation that we used to transform the body mass matrix.

$$M_{A,i}^{b} = \begin{bmatrix} \mathbb{I}_{3\times3} & [0]_{3\times3} \\ S(\mathbf{r}_{cg_i}^{b}) & \mathbb{I}_{3\times3} \end{bmatrix} M_{A,i}^{cg_i} \begin{bmatrix} \mathbb{I}_{3\times3} & S^{\top}(\mathbf{r}_{cg_i}^{b}) \\ [0]_{3\times3} & \mathbb{I}_{3\times3} \end{bmatrix} \tag{4.20}$$

where:

$M_{A,i}^{b}$ is the added mass of part i at total mass reference frame (F_b)

$M_{A,i}^{cg_i}$ is the added mass of part i at F_{cg_i}

Lastly, the total added mass matrix is computed from the summation of the transform coordinate added mass matrix specify in (4.20)

$$\begin{aligned} M_{A,total}^{b} &= \sum_{i} M_{A,i}^{b} \\ &= \begin{bmatrix} 2.3003 & 0 & 0 & 0 & 0.1791 & 0 \\ 0 & 61.5339 & 0 & 0.4033 & 0 & 1.4278 \\ 0 & 0 & 85.3640 & 0 & 12.8568 & 0 \\ 0 & 0.4033 & 0 & 0.1055 & 0 & 0.3974 \\ 0.1791 & 0 & 12.8568 & 0 & 19.6375 & 0 \\ 0 & 1.4278 & 0 & 0.3974 & 0 & 10.4835 \end{bmatrix} \end{aligned} \tag{4.21}$$

4.2.4 Added mass comparisons

In this section, we compare the effect of the added mass of each part to the total added mass of the system. The comparison is done by finding the percentage of each element in the added mass matrix. The comparison that will be done in this section consist of

- The effect of the added mass from the modem 1, modem 2, antenna, charger on the total added mass.

$$\%m_{A,i} = \left| \frac{m_{A_{mod},i}}{m_{A_{orig},i}} \right| \times 100 \tag{4.22}$$

where:

$m_{A_{mod}}$ is the total added mass without modem 1, modem 2, antenna and charger

$m_{A_{orig}}$ is the total added mass

$$M_{A_{mod}} = \begin{bmatrix} 0.9055 & 0 & 0 & 0 & 0.2070 & 0 \\ 0 & 3.3003 & 0 & -0.7614 & 0 & -1.4564 \\ 0 & 0 & 0.2557 & 0 & 0.1196 & 0 \\ 0 & -0.7614 & 0 & 0.1774 & 0 & 0.3397 \\ 0.2070 & 0 & 0.1196 & 0 & 0.1195 & 0 \\ 0 & -1.4564 & 0 & 0.3397 & 0 & 0.7061 \end{bmatrix} \tag{4.23}$$

$$\begin{aligned} \%m_{A,11} &= 39.3637 \\ \%m_{A,22} &= 5.3635 \\ \%m_{A,33} &= 0.2995 \\ \%m_{A,44} &= 168.1055 \\ \%m_{A,55} &= 0.6083 \\ \%m_{A,55} &= 6.7356 \end{aligned} \tag{4.24}$$

As we can see from the (4.24) that even though the shapes are small, in some part it could affect the total added mass of the system. For example, the $m_{A,44}$ where the added is changed a lot compared to other part, such as $m_{A,22}$ and $m_{A,33}$ where the added mass of the main body significantly dominate the value.

4.3 Drag Matrices

The friction force is a type of force that results from a body that moves inside a fluid region. Friction force creates a damping effect, which counters the translational/angular forces of the moving body. This force is mainly caused by the presence of skin friction, wave drift damping, damping due to vortex shedding, lifting forces, and other viscous effects. Due to the complexity of the calculation process, the drag coefficient is introduced to better estimate the friction forces by using the characteristic width, length, projected surface, and shape of the moving body.

The drag coefficient matrix ($M_D \in \mathbb{R}^{6\times6}$) contains coefficients to compute the friction force of the AUV component. The drag coefficients matrix can be written like this:

$$D_{Rb}^{CB} = \begin{bmatrix} K_{11} & 0 & 0 & 0 & 0 & 0 \\ 0 & K_{22} & 0 & 0 & 0 & 0 \\ 0 & 0 & K_{33} & 0 & 0 & 0 \\ 0 & 0 & 0 & K_{44} & 0 & 0 \\ 0 & 0 & 0 & 0 & K_{55} & 0 \\ 0 & 0 & 0 & 0 & 0 & K_{66} \end{bmatrix} \tag{4.25}$$

The local coordinate system originated in the buoyancy centre of the body. Each component of the matrix is defined as:

$K_{11} = \frac{1}{2}\rho S_x C_{D11}$ with S_x and C_{D11} are the projected surface and the 3D drag coefficient in the $\vec{x}$ direction.

$K_{22} = \frac{1}{2}C_{D22}D_y L$ with D_y and C_{D22} are the characteristic width and the 2D drag coefficient in the $\vec{y}$ direction.

$K_{33} = \frac{1}{2}C_{D33}D_z L$ with D_z and C_{D23} are the characteristic width and the 2D drag coefficient in the $\vec{z}$ direction.

$K_{44} = 0$

$K_{55} = \frac{1}{64}\rho L^4 C_{D33} D_z$

$K_{66} = \frac{1}{64}\rho L^4 C_{D22} D_y$

Below will be listed all the drag coefficient matrix for each component of the Sparus AUV:

1. $D_{MainBody} = \begin{bmatrix} 8.31 & 0 & 0 & 0 & 0 & 0 \\ 0 & 200.83 & 0 & 0 & 0 & 0 \\ 0 & 0 & 200.83 & 0 & 0 & 0 \\ 0 & 0 & 0 & 0 & 0 & 0 \\ 0 & 0 & 0 & 0 & 28.26 & 0 \\ 0 & 0 & 0 & 0 & 0 & 28.26 \end{bmatrix}$

2. $D_{Modem1} = \begin{bmatrix} 0.29 & 0 & 0 & 0 & 0 & 0 \\ 0 & 0.29 & 0 & 0 & 0 & 0 \\ 0 & 0 & 0.46 & 0 & 0 & 0 \\ 0 & 0 & 0 & 0 & 0 & 0 \\ 0 & 0 & 0 & 0 & 0 & 0 \\ 0 & 0 & 0 & 0 & 0 & 0 \end{bmatrix}$

3. $D_{Modem2} = \begin{bmatrix} 0.69 & 0 & 0 & 0 & 0 & 0 \\ 0 & 0.69 & 0 & 0 & 0 & 0 \\ 0 & 0 & 0.49 & 0 & 0 & 0 \\ 0 & 0 & 0 & 0 & 0 & 0 \\ 0 & 0 & 0 & 0 & 0 & 0 \\ 0 & 0 & 0 & 0 & 0 & 0 \end{bmatrix}$

4. $D_{Antenna} = \begin{bmatrix} 9.16 & 0 & 0 & 0 & 0 & 0 \\ 0 & 15.83 & 0 & 0 & 0 & 0 \\ 0 & 0 & 2.26 & 0 & 0 & 0 \\ 0 & 0 & 0 & 0 & 0 & 0 \\ 0 & 0 & 0 & 0 & 0.002 & 0 \\ 0 & 0 & 0 & 0 & 0 & 0.005 \end{bmatrix}$

5. $D_{ChargingPort} = \begin{bmatrix} 0.1719 & 0 & 0 & 0 & 0 & 0 \\ 0 & 0.6745 & 0 & 0 & 0 & 0 \\ 0 & 0 & 1.349 & 0 & 0 & 0 \\ 0 & 0 & 0 & 0 & 0 & 0 \\ 0 & 0 & 0 & 0 & 0 & 0 \\ 0 & 0 & 0 & 0 & 0 & 0 \end{bmatrix}$

6. $D_{ThrusterLeft} = \begin{bmatrix} 4.32 & 0 & 0 & 0 & 0 & 0 \\ 0 & 6.93 & 0 & 0 & 0 & 0 \\ 0 & 0 & 6.93 & 0 & 0 & 0 \\ 0 & 0 & 0 & 0 & 0 & 0 \\ 0 & 0 & 0 & 0 & 0.003 & 0 \\ 0 & 0 & 0 & 0 & 0 & 0.003 \end{bmatrix}$

From the drag coefficient above, we can see the behaviour of the drag force on the component. For the main body drag coefficient, movement in the y and z direction will create a much bigger friction force due to the big difference in the projected surface area. Minor parts such as modem 1, modem 2, and the charging port, contribute a relatively low contribution to the friction forces and moment. However, it is a different case for the antenna. Because of the height of this component, it contributes a rather significant friction force and a small amount of turning moment (but still present. Even though the presence of modem 1, modem 2, and the charging port might not be that significant to create significant friction forces, it is important to consider including the antenna for the modelisation process.

The friction forces work on the buoyancy centre of the moving body. Because of that, we have to compute the velocity at the buoyancy centre of each body from the velocity measured at the DVL position to get the friction forces. To do that we will use the transformation matrix H as show below:

$$V^b_{b_i/n} = H(C_{\vec{DVL}}b_i)V^b_{C_{DVL}/n} \tag{4.26}$$

The global drag force of a body expressed on its buoyancy centre b_i can then be calculated using the formula:

$$\tau^b_{b_i,i} = K^{b_i}_{q,i} * |V^b_{b_i/n}| * V^b_{b_i/n} \tag{4.27}$$

Then we compute the global friction force $\tau^b_{b_i,i}$ to the gravity centre of the reference body. To do that we apply the transformation matrix H^T, and we get:

$$\tau^b_{g_0,i} = H^T(g_0\vec{b}_i)\tau^b_{b_i,i} \tag{4.28}$$

In Chapter 5, the effect of the friction forces of each component will be further explained by implementing some simulations. This will help to further support our argument about our drag coefficient matrix.

Chapter 5

Simulation

In this chapter, we will discuss the result from a simulation of the Sparus AUV. From this result, we will see how the Sparus AUV behaves given the parameters and input force in the form of propulsion thrust. The behaviour of the Sparus AUV will be defined by observing the change of state x, y, z, ϕ, θ, ψ, u, v, w, p, q, r, $\dot{u}$, $\dot{v}$, $\dot{w}$, $\dot{p}$, $\dot{q}$, & $\dot{r}$. We are also going to compare it to Sparus AUV when the attached appendages are ignored. The input forces will be a small thrust (5 %) for the left and right thrusters, while the vertical thruster will remains off.

5.1 Position Comparison

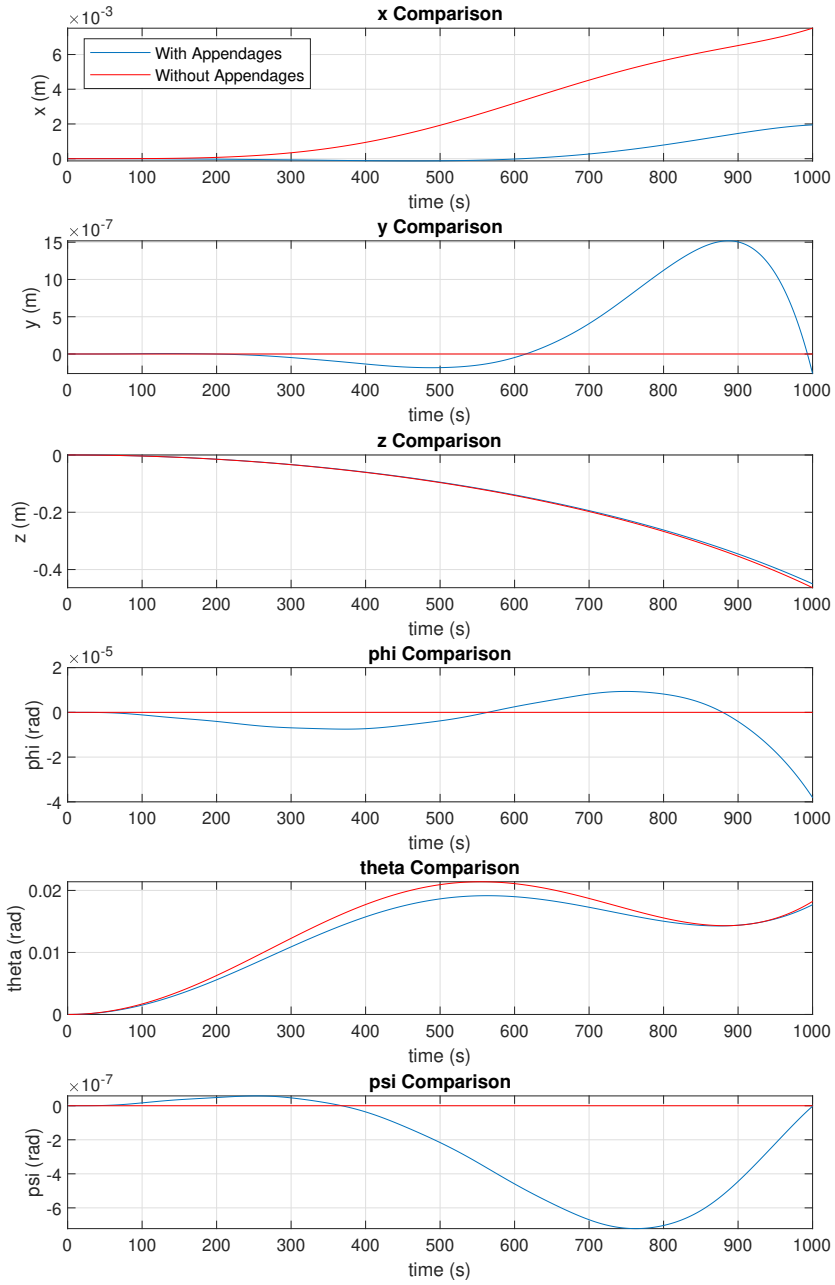

Figure 5.1: Simulated Position Comparison

From the x position, we can see that movement in the direction of AUV with appendages is strongly inhibited by the presence of the appendages. While in the y direction, the AUV with appendages seems to have some small movement initially but becomes greater as times continue.

Movement in the z-direction is relatively the same, and it is descending due to the gravitational force and the absence of the vertical thrust. For the angular movement ϕ (roll) and ψ (yaw), we see some disturbance for the AUV with appendages. While the pitch movement θ, is relatively the same for both AUV with and without appendages the AUV without appendages does have a slightly bigger movement.

5.2 Velocity Comparison

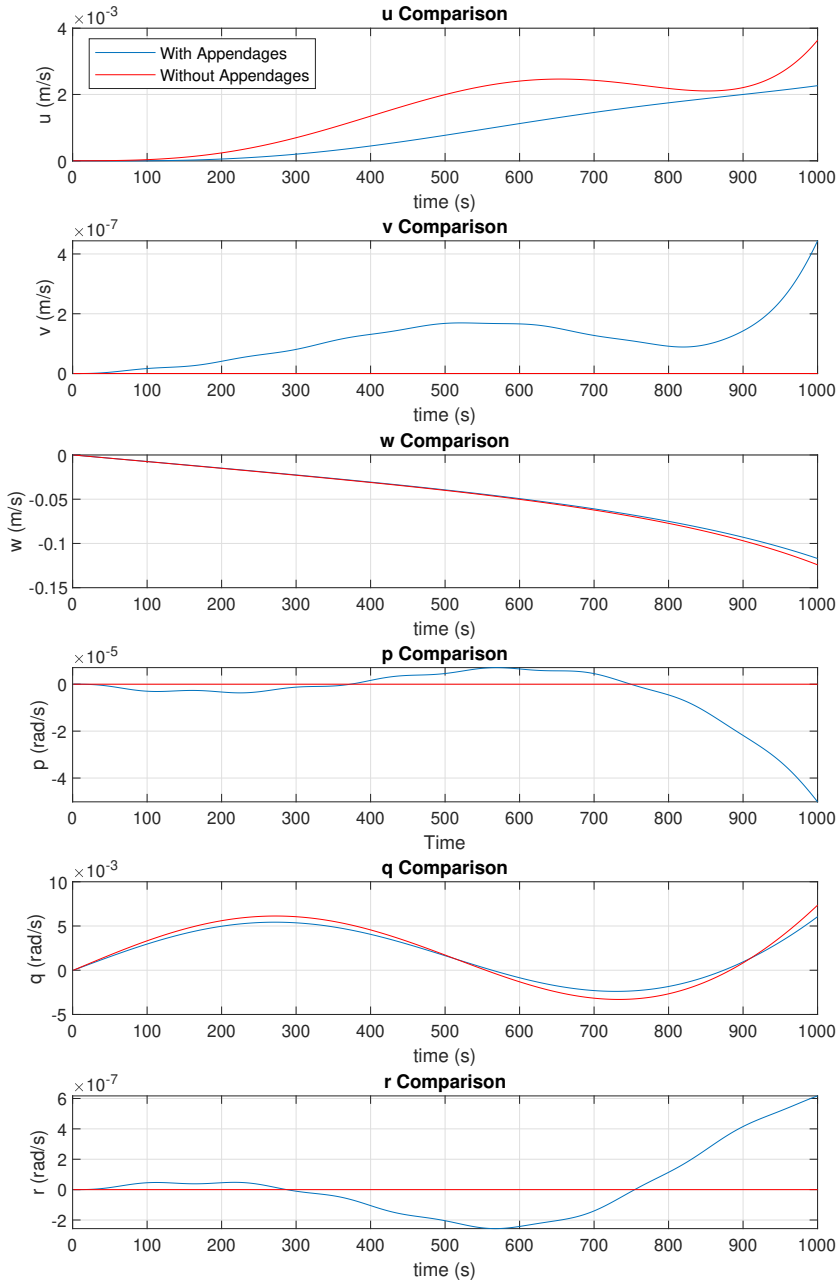

Figure 5.2: Simulated Velocity Comparison

For the velocity in the x direction, we also see the same pattern with the positional change in the x direction. There is a sign of a damping occurrence in the AUV with appendages. As for the velocity in the y direction, It is shown that the v velocity is growing significantly at the

end of the simulation. This could happen because the presence of an antenna causes instability as the AUV moves. The vertical velocity and pitch angular velocity remain similar with a slight difference between the two. While the roll and yaw velocity observed still show a significant change at the end of the simulation

5.3 Acceleration Comparison

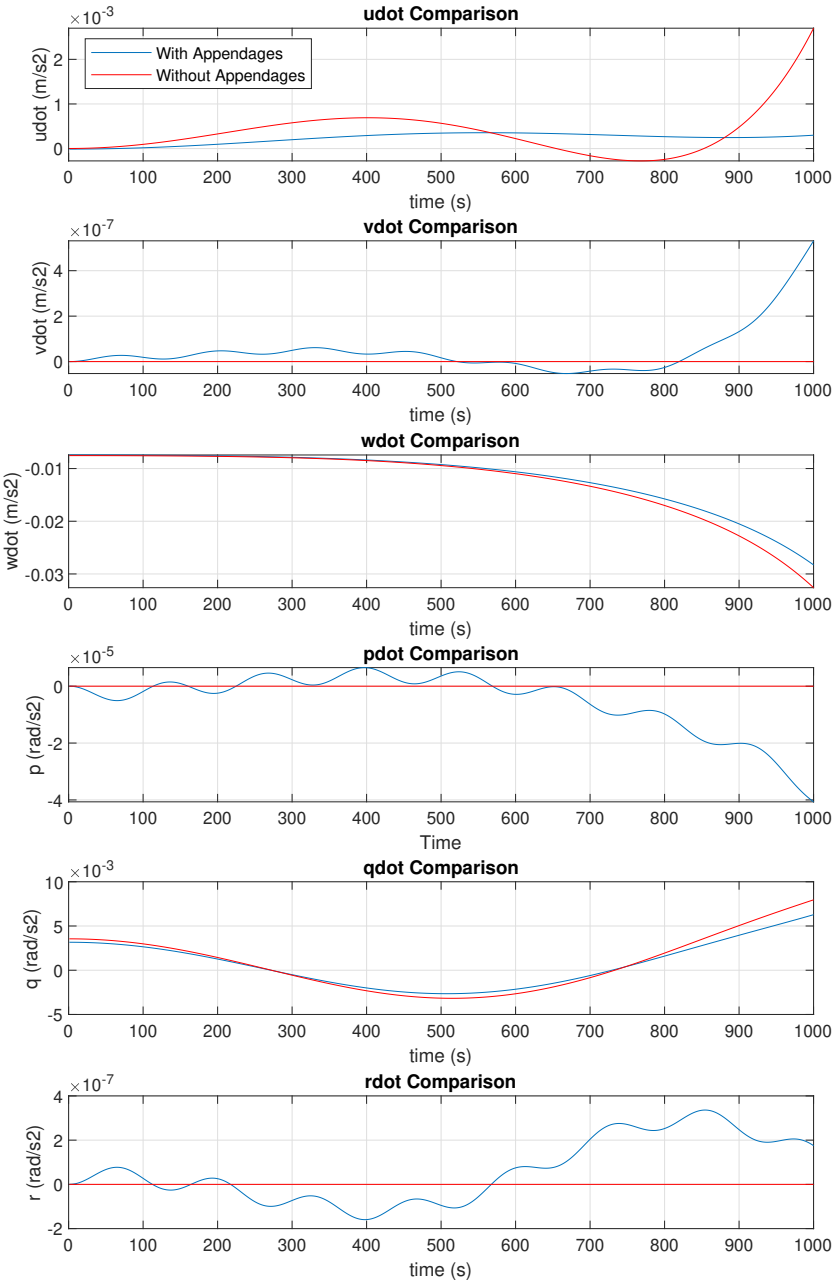

Figure 5.3: Simulated Acceleration Comparison

Acceleration in the x direction for the AUV without appendages at first is increasing, but then suddenly decreases and finally able to recover and increase, while for the acceleration of the AUV with appendages seems to be stagnant at the end of the simulation. Acceleration at

y direction and angular acceleration for yawing movement shows an oscillatory type of change. This shows that even when moving in the x direction, an underwater vehicle with a lot of appendages can show instability in another axis of movement. The acceleration in the z-direction for both AUVs with and without appendages shows an exponential increase due to gravity. The pitch angular velocity also shows a similar change for both AUVs.